Almeida, RSM, Bergmüller, EL, Lührs, H, et al.

Thermal exposure effects on the long-term behavior of a mullite fiber at high temperature

Recommended Citation (primary publication/Version of Record) incl. DOI:

Almeida, RSM, Bergmüller, EL, Lührs, H, et al. Thermal exposure effects on the long-term behavior of a mullite fiber at high temperature. J Am Ceram Soc. 2017; 100: 4101–4109. https://doi.org/10.1111/jace.14922

Take down policy
If you believe that this document or any material on this site infringes copyright, please contact publizieren@suub.uni-bremen.de with full details and we will remove access to the material.

Thermal exposure effects on the long-term behavior of a mullite fiber at high temperature

Renato S. M. Almeida[1] | **Eduardo L. Bergmüller[1]** | **Hanna Lührs[2]** (iD) |
Michael Wendschuh[3] | **Bernd Clauß[4]** | **Kamen Tushtev[1]** (iD) | **Kurosch Rezwan[1,2]**

[1]Advanced Ceramics, University of Bremen, Bremen, Germany

[2]MAPEX - Center for Materials and Processes, University of Bremen, Bremen, Germany

[3]Department of Geosciences, University of Bremen, Bremen, Germany

[4]Institute of Textile Chemistry and Chemical Fibers, Denkendorf, Germany

Correspondence
Kamen Tushtev, Advanced Ceramics, University of Bremen, Bremen, Germany.
Email: tushtev@uni-bremen.de

Abstract

The behavior of an oxide fiber at elevated temperatures was analyzed before and after thermal exposures. The material studied was a mullite fiber developed for high-temperature applications, CeraFib 75. Heat treatments were performed at temperatures ranging from 1200°C to 1400°C for 25 hours. Quantitative high-temperature X-ray analysis and creep tests at 1200°C were carried out to analyze the effect of previous heat treatment on the thermal stability of the fibers. The as-received fibers presented a metastable microstructure of mullite grains with traces of alumina. Starting at 1200°C, grain growth and phase transformations occurred, including the initial formation of mullite, followed by the dissociation of the previous alumina-rich mullite phase. The observed transformations are continuous and occur until the mullite phase reaches a state near the stoichiometric 3/2 mullite. Only the fibers previously heat treated at 1400°C did not show further changes when exposed again to 1200°C. Overall, the heat treatments increased the fiber stability and creep resistance but reduced the tensile strength. Changes observed in the creep strain *vs*. time curves of the fibers were related to the observed microstructural transformations. Based on these results, the chemical composition of the stable mullite fiber is suggested.

KEYWORDS
creep, fibers, heat treatment, microstructure, mullite

1 | INTRODUCTION

Over the past decades, ceramic matrix composites (CMCs) based on only oxide materials (Ox-CMCs) have been developed. Even though their development is considerably recent, these materials have already achieved a level of maturity for use in different industrial sectors, such as aerospace, power generation, hot gas filtration and metallurgical heat treatment.[1,2] This growing interest in Ox-CMCs is due to their natural chemical stability, coupled with their high strength and considerable toughness, which is well known from CMCs.[3,4] Logically, the development and production of such oxide systems was only possible due to the commercialization of high-strength oxide fibers. The first commercial oxide fibers were released in the 70s, but these fibers were rather fragile when handled and presented very low thermal stability.[5] Only in the 90s were suitable oxide fibers commercialized, which allowed the further progress of Ox-CMCs.[3] The current development of Ox-CMCs is mainly related to fibers commercialized by the American company Minnesota Mining and Manufacturing (3M, Minnesota, USA): the alumina fiber Nextel 610, known as the strongest oxide fiber at room temperature, and the mullite-based fiber Nextel 720, credited to have the highest creep resistance.[6]

Nevertheless, attention should be given to the high-temperature behavior of oxide fiber composites, since they are

prone to creep and loss of strength when exposed to temperatures above 1000°C.[7-10] This indicates that used oxide fibers are subject to thermal degradation. Taking Nextel 720 as an example, several studies have been conducted on its creep performance, and it was shown that this fiber can exhibit high creep deformation at 1200°C.[6,11-13] A decrease in strength was also reported after exposure to the same temperature,[14] due to grain growth[15,16] and grain-boundary grooving.[17] Therefore, the development/improvement of fibers that can overcome these limitations is of great interest. Therefore, the Institute of Textile Chemistry and Chemical Fibers (ITCF, Denkendorf, Germany), together with the German company CeraFib GmbH (Olbersdorf, Germany), has produced the nearly pure mullite fiber Cera-Fib 75. At the current state of development, this fiber shows a lower room-temperature strength than Nextel 720 but higher strength retention at temperatures above 1200°C.[13,18]

As discussed above, the exposure of oxide fibers to temperatures above 1000°C is of great concern. It should also be noted that such temperatures are normally reached during the processing of CMCs, as well as during their in-field usage. It is generally agreed upon in the literature that prolonged exposure to high temperatures should be avoided, since exposure leads to fiber grain growth and decreased tensile strength. Nevertheless, other microstructural changes, besides grain growth, also occur during the heat treatment of oxide fibers, especially in two-phase fibers such as Nextel 720 and CeraFib 75. In our previous study[18], it was shown that both mullite fibers undergo crystalline phase changes after heat treatment, leading to a more stable microstructure. It can thus be expected that the fibers will have higher thermal stability after exposure and, as a consequence, higher creep resistance. Studies on the creep behavior of heat-treated oxide fibers are quite rare and typically concern only alumina-based fibers.[19,20] Hence, the objective of this work is to analyze the influence of previous thermal exposure on the long-term behavior of the fiber CeraFib 75 at high temperatures. To this end, the fibers were heat treated at temperatures between 1200°C and 1400°C for 25 hours and then characterized. The analysis was done in two steps. First, high-temperature X-ray diffraction (XRD) analyses were conducted to quantify the phase transformations over time at 1200°C. Second, the long-term behavior of the fibers under load was analyzed with several creep tests at the same temperature.

2 | EXPERIMENTAL PROCEDURE

2.1 | Materials

All experiments were conducted on the mullite fiber Cera-Fib 75. This 10 μm fiber is produced by a dry-spinning process, using a solution containing 72 wt% alumina and 28 wt% silica. Due to volatilization of the Si species, the fiber composition after pyrolysis is of approximately 75 and 25 wt%, respectively. The fiber exhibits a microstructure of mullite grains with traces of γ-alumina. Further details/properties of the fiber have been published elsewhere.[13] For the methodology described below, fibers were tested before (as-received) and after heat treatment for 25 hours at temperatures of 1200°C (HT 1200), 1300°C (HT 1300) and 1400°C (HT 1400). The heat-treatment duration of 25 hours was set in accordance to previous studies, as microstructural changes were observed within this time.[18] All thermal exposures were conducted in a Nabertherm LHT 04/17 chamber furnace (Nabertherm GmbH, Lilienthal, Germany).

2.2 | Characterization methods

To obtain an overview of the changes caused by thermal exposure, the as-received and heat-treated fibers were characterized in relation to their microstructure. Microstructural observations were obtained, using scanning electron microscopy (SEM). For this, the fibers were initially embedded in epoxy resin to prepare the surface, i.e., by grinding and polishing. Subsequently, the epoxy resin was thermally extracted, and the prepared fibers were thermally etched at 1300°C for 30 minutes. Micrographs of the fibers were taken using a ZEISS Supra 40 SEM (ZEISS, Oberkochen, Germany) with an acceleration voltage of 0.5 kV. Grain size measurements were done, using the intercept line method with the help of the Lince software (TU Darmstadt, Germany). A total of five fibers per condition were analyzed.

2.3 | High-temperature X-ray diffraction

To study the influence of the previous thermal exposure on the phase transformation at 1200°C, in situ high-temperature XRD experiments were performed on the as-received and heat-treated samples. High-temperature XRD is a useful tool to study the kinetics of these transformations, which can also influence the creep performance of the fibers. Sample preparation consisted of crushing the fiber bundles to a fine powder. Measurements were performed using a Bragg-Brentano PANalytical X'Pert MPD PRO diffractometer (PANalytical GmbH, Kassel-Waldau, Germany), equipped with a high-temperature chamber HTK1200N (Anton Paar, Vienna, Austria), using Cu$K_{\alpha 1,2}$ radiation, a Ni beta filter, and a X'Celerator detector system. Data were collected from 2θ=5 to 120° with a total measuring time of 46 minutes for each scan. During the heating phase, scans were performed at constant temperatures of room temperature, 200°C, 400°C, 600°C, 800°C,

and 1000°C. The samples were then kept at 1200°C for approximately 8 hours with continuous collection of 11 diffraction patterns. Phase quantification was obtained by Rietveld refinements, using the Diffracplus Topas 4.2 software (Bruker AXS GmbH, Karlsruhe, Germany). After careful refinement of the diffraction patterns recorded at room temperature, the resulting parameters were used as a starting model for the refinement of the patterns recorded at elevated temperatures. The following parameters were refined for all diffraction patterns: 6 background coefficients (Chebychev polynomial), zero-point error and sample displacement, in order to account for the thermal expansion of the sample holder. For all phases, the lattice parameters and scale factors were refined, and only for the major phase (mullite) were the Lorentzian crystallite size parameters optimized. For reference, R-values are given in the Table S1 and S2, which is available on line.

2.4 | Creep tests

Single-filament tensile creep tests were performed to analyze the long-term behavior of the as-received and heat-treated fibers under load at 1200°C. To do so, the fibers were manually separated from the fiber bundle, using surgical gloves. The fiber filaments were tested using a dead load system and a two SiC heating element oven. The specimens were heated at a rate of 1°C/s, and the target temperature was held for approximately 15 minutes before the load was slowly released. The samples were tested until failure or until reaching the run-out time of 50 hours. This run-out time was chosen based on previous studies, as the fibers reach the secondary creep stage within this time.[13] Three different weights were used to apply different creep loads. After the tests, the diameter of each tested fiber was measured on a SENSOFAR PLμ 2300 optical microscope (Sensofar Group, Terassa, Spain) to calculate the applied stress. To calculate the creep strain, an effective gauge length of 11.0 mm was determined, following the methodology proposed by Morrell.[21] Furthermore, the fracture surfaces of the tested fibers that failed before the run-out time were analyzed, using SEM.

3 | RESULTS

3.1 | Room-temperature properties

The effect of the heat treatments on the room-temperature properties of the fibers was examined by microstructural observations. Figure 1 presents the evolution of the microstructure of the fibers after the different heat treatments were performed. The microstructure of these fibers has been described previously.[18] With the improved grinding and polishing technique, the micrographs presented below show a much higher quality, allowing for a better interpretation of the fiber microstructure. In addition, the contrast of the figures was enhanced to identify the grain boundaries. The as-received CeraFib 75 fiber showed a microstructure of mostly equiaxial mullite grains of approximately 175 nm. Changes
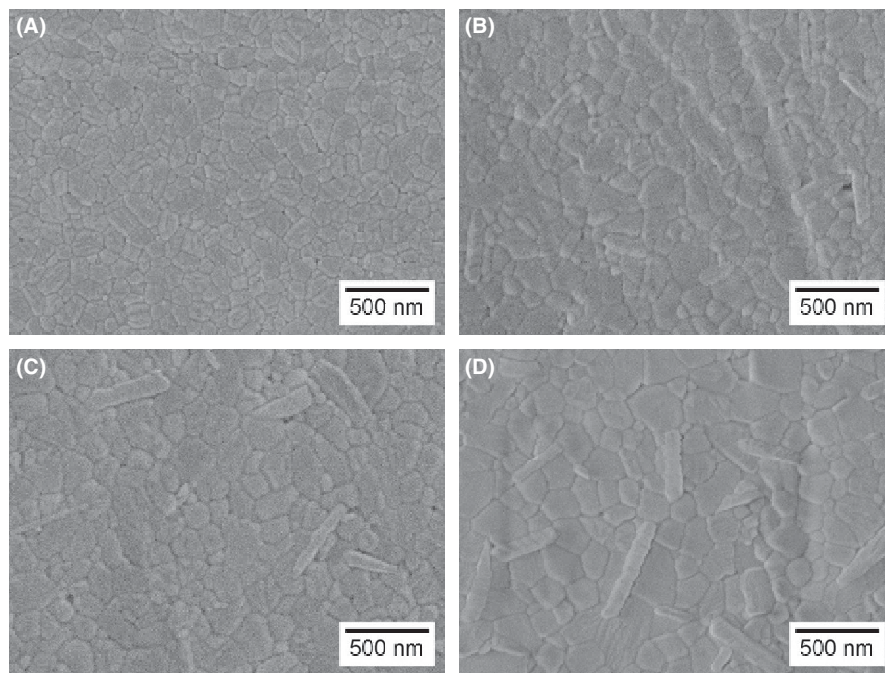

FIGURE 1 Microstructural evolution of CeraFib 75: as-received fiber (A) and fibers after heat treatment for 25 hours at temperatures of 1200°C (B), 1300°C (C) and 1400°C (D)
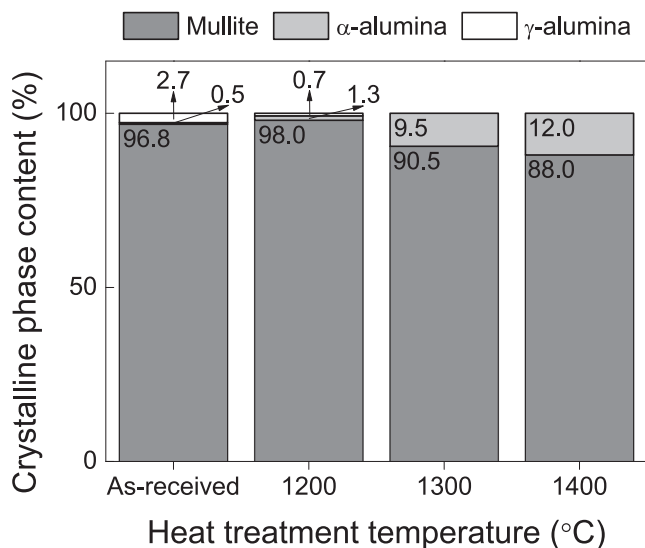
FIGURE 2 Crystalline phase quantification by XRD at room temperature for the as-received fibers and the fibers after heat treatment for 25 hours at temperatures of 1200°C-1400°C

in the grain size were seen after exposure to 1200°C, at which the grains enlarged to 235 nm. Further changes were observed at 1300°C, with grains on the order of 260 nm and some being more elongated. After exposure to 1400°C, several elongated grains were detected, presumably of alumina, and the grains were on average 370 nm.

Room-temperature XRD measurements gave further information regarding the microstructural changes caused by heat treatment. Quantification of the crystalline phases of the as-received and heat-treated fibers is given in Figure 2. These results were obtained with the same measuring parameters as used in the high-temperature XRD analysis for comparison and show the same tendency as seen in results published previously.[18] Before heat treatment, the fiber is mainly composed of mullite with traces of the γ-alumina phase. Again, changes were seen upon heat treatment at 1200°C, after which the amount of γ-alumina decreased, while the amount of both α-alumina and mullite slightly increased. At higher temperatures, HT 1300 and HT 1400, the ratio of the α-alumina phase increased, while that of the mullite phase decreased, indicating the dissociation of mullite, as discussed previously.[18]

3.2 | High-temperature XRD analysis

Based on the quantitative phase composition obtained from Rietveld refinement of the in situ high-temperature XRD experiments, information about the phase transformation kinetics at 1200°C were gained. The phase quantifications of the as-received and HT 1400 samples at all applied temperatures are displayed in Figure 3, where the vertical line separates the heating phase (left) from the continuous measurements at 1200°C (right). It should be noted that since
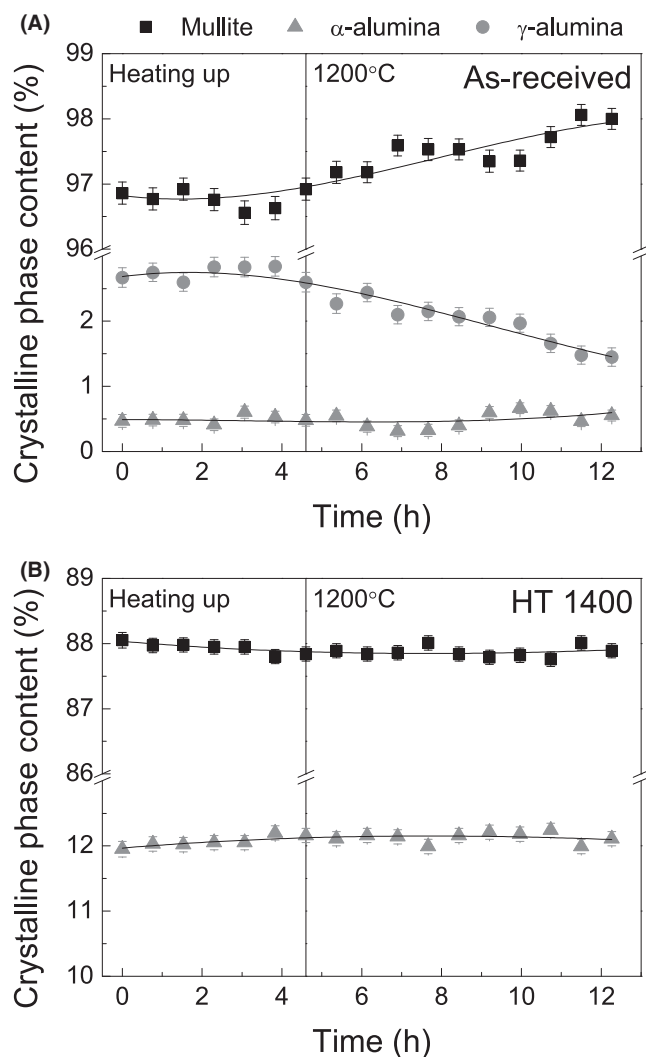

FIGURE 3 Crystalline phase quantification by XRD at high temperature for the as-received fibers (A) and the fibers after heat treatment for 25 hours at the temperature of 1400°C (B). Measurements were performed at defined temperatures during heating to 1200°C (left) and continuously at the temperature of 1200°C (right). During the measurements, the temperature was kept constant

each sample yielded a different crystalline phase content (see Figure 2), different ranges were used in the graphs in Figure 3, but they have the same scale. The results for the HT 1200 and HT 1300 fibers are not presented, as their refinement resulted in relatively high data scattering and only small changes were observed. For instance, a small decrease in the mullite content was observed for both samples when comparing the measurements at room temperature to the ones at 1200°C: 98.0 wt% to 97.2 wt% and 90.5 wt% to 89.9 wt% for the HT 1200 and HT 1300 fibers, respectively. Then again, these changes are in the limit of the method, and a proper interpretation of the data cannot be made due to the scattering between the results.

The as-received CeraFib 75 fiber, shown in Figure 3A, was the most sensitive to crystalline phase transformation

at 1200°C. During the heating phase, no significant changes of the phase composition were observed. In contrast, the diffraction patterns recorded during the 8 hours period at 1200°C revealed distinct transformations of the crystalline phase. Considering the as-received state, the γ-alumina phase content decreased from 2.7 wt% to 1.4 wt%, while the mullite content increased from 96.8 wt% to 98.1 wt% after only 8 hours at 1200°C. On the other hand, the amount of α-alumina phase remained constant at 0.5 wt % within the duration of the scans. It can be expected that if the experiments were conducted for 25 hours at 1200°C, the fiber would then present the composition of the HT 1200 fibers: 98.0 wt% mullite, 1.3 wt% α-alumina, and 0.7 wt% γ-alumina. Unfortunately, as 1200°C represents the highest possible operating temperature of the equipment, an extension of the experiment was not considered.

For the samples heat treated at 1400°C, no significant differences were seen during the high-temperature measurements (Figure 3B). Hence, it can be concluded that the fibers achieved higher stability after exposure to 1400°C, and therefore, no crystalline changes were seen when the fiber was again exposed to a lower temperature of 1200°C.

3.3 | Creep tests

Figure 4 presents examples of the creep tests of the as-received and heat-treated fibers under three different loads at 1200°C. The graphs are plotted until 20 hours for better

visualization of the tests with the highest creep load. It is important to note that the creep tests were performed at the same temperature as the high-temperature XRD measurements. In general, the tested fibers showed a nonlinear region, primary creep stage, followed by a constant creep rate, secondary creep stage. A tertiary creep stage was not observed, which is expected given that the fibers are brittle. By comparing the results of the as-received fibers with the results of the heat-treated fibers, the effect of the previous thermal exposure was evident. In summary, a higher heat-treatment temperature results in fibers that are more creep resistant, i.e., the fibers exhibit a lower creep rate and longer creep lifetime. Nevertheless, this higher creep resistance comes at the expense of the tensile strength of the material. For instance, the HT 1400 fibers could not be tested with the highest load since they failed during loading, before the test began. In the same manner, the strain to failure decreased with an increase in the treatment temperature, e.g., the HT 1300 specimen tested with 306 MPa broke with a strain to failure of only 0.11%, while the as-received and HT 1200 samples could undergo a creep deformation of 0.2% or more before failure. Another aspect of the creep tests that should be highlighted is the duration of the primary creep stage. For stresses below 230 MPa, the as-received and HT 1200 specimens presented a much longer nonlinear span of almost 4 hours. The fibers heat treated at 1300°C showed a primary creep stage of approximately 2.5 hours under the same conditions, while the
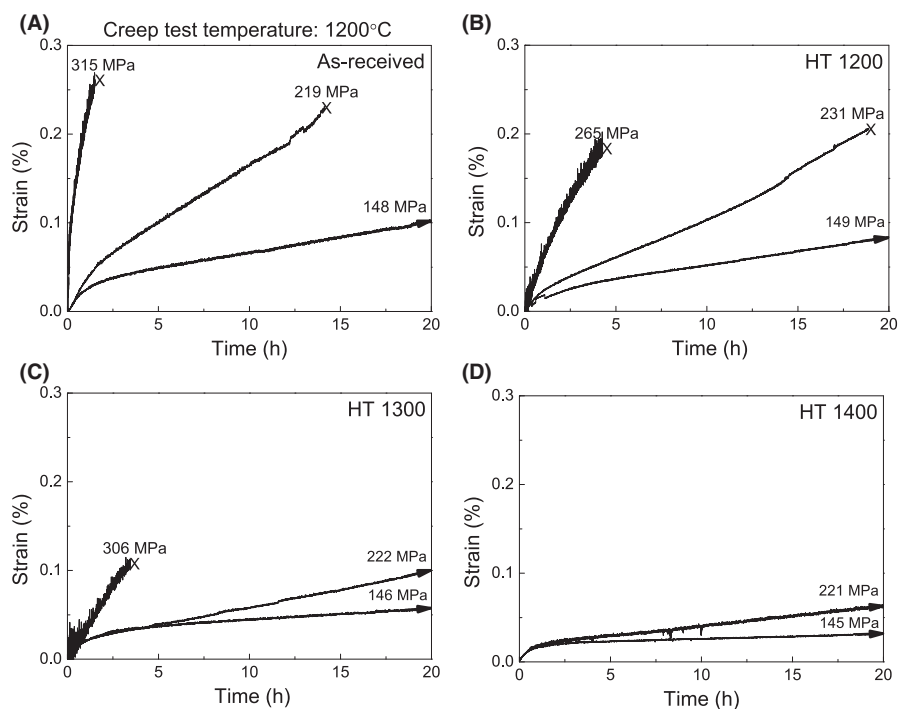

FIGURE 4 Creep deformation vs time for the CeraFib 75 fibers tested at 1200°C under different applied stresses. Tests were performed on the as-received fibers (A) and the fibers after heat treatment for 25 hours at temperatures of 1200°C (B), 1300°C (C) and 1400°C (D). Arrows indicate that the samples did not fail in the given run-out time
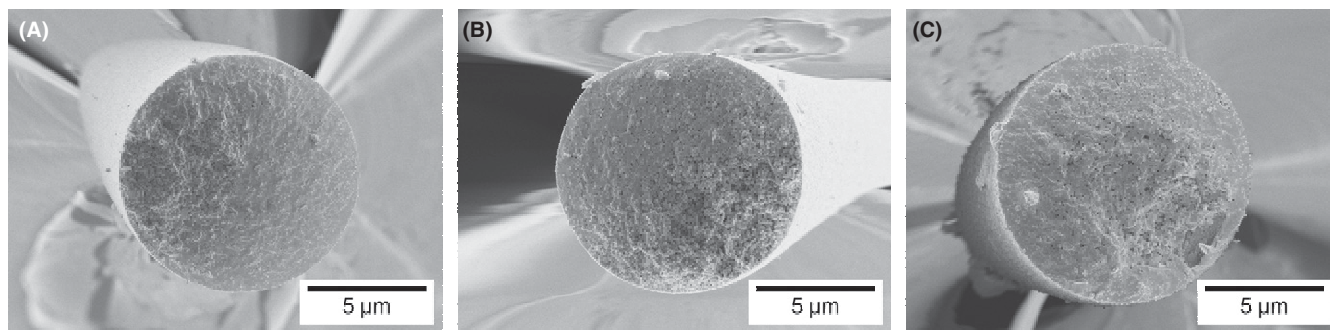
FIGURE 5 Fracture surface of the fibers tested under creep loading at 1200°C: as-received fiber tested with a stress of 315 MPa (A), HT 1200 fiber tested with a stress of 265 MPa (B) and HT 1300 fiber tested with a stress of 306 MPa (C)

creep rate of HT 1400 remained constant after only 1.5 hours.

Further differences were observed when analyzing the fracture surfaces of the crept fibers (Figure 5). The failure of the as-received fibers, as shown in Figure 5A, presumably began on the surface. In this region, crack propagation was initially intergranular, followed by a planar intragranular failure along the remaining portion of the fiber. The HT 1200 fibers failed in a similar manner, as shown in Figure 5B, although the depicted fiber has a larger intergranular region. In addition, the fiber also showed signs of cavitation, represented by the black dots in the figure. On the other hand, the fracture surface, shown in Figure 5C for an HT 1300 fiber, has a much different aspect. The fiber presents a considerable amount of cavities. Hence, it is suggested that the failure of the fiber began in the middle due to the coalescence of these cavities. As the remaining cross-section of the fiber could no longer sustain the creep load, a planar failure was then observed along the outer perimeter of the fiber. The fracture surface of HT 1400 fibers is not depicted in Figure 5 since the fibers survived the 50 hours run-out time.

4 | DISCUSSION

As discussed above, heat treatment caused different microstructural changes, which in turn affected the mechanical and long-term properties of the fibers. The main changes observed were grain growth and crystalline phase transformations. The grain growth kinetics of mullite fibers was studied in detail by Schmücker.[14,22] In his works, it was shown that other mullite fibers also present grain growth starting at 1200°C but with overall slow kinetics at temperatures below 1600°C. In CeraFib 75, the low mobility of the mullite grains resulted in only slight grain coarsening at 1200°C, as shown in Figure 1B. At higher temperatures, the content of α-alumina grains increased significantly, as shown in Figure 2, and changes in the grain

size and morphology were more evident, as shown in Figure 1C,D. As shown in our previous study on fiber bundles, this grain growth is responsible for the loss of room-temperature strength observed for the treated fibers.[18]

The second microstructural change observed after heat treatment was related to crystal phase transformations, which were analyzed in more detail through the high-temperature XRD measurement of the as-received sample, as shown in Figure 3A. Because of the short pyrolysis time during its manufacturing, as-received CeraFib 75 fibers have a metastable microstructure of alumina-rich mullite and traces of γ-alumina. This microstructure is considerably stable up to 1200°C, at which it will gradually transform to the state of least energy. Within the first hours at 1200°C, the γ-alumina content decreased, and the mullite content increased. Previous studies have indicated that the fiber may contain an amorphous silica phase in amounts lower than 1 wt%,[18] which enables the formation of mullite in combination with the γ-alumina phase. This reaction occurs until the amorphous silica is completely consumed, which is likely to occur shortly after the 8 hours at 1200°C, last XRD measurement in Figure 3A. From that point on, the remaining γ-alumina phase transforms into α-alumina, as this phase is the most stable one.[23] Although it is not evident from the high-temperature XRD measurements of the as-received fibers, the higher amount of α-alumina in the HT 1200 fibers suggests that the dissociation of mullite into α-alumina also occurs at 1200°C. As stated before, the mullite present in the as-received fibers is in a metastable state and rich in Al. Presumably after the formation of mullite from γ-alumina and free silica, the as-received mullite phase will dissociate into α-alumina and mullite with a lower content of Al. This dissociation is time dependent, and the reaction is not completed within the first 25 hours of exposure to 1200°C. Thus, when the heat-treated fibers are heated again, the mullite further dissociates.

Since the phase transformations described above are thermally activated processes, they will occur faster at higher temperatures. Hence, the fibers heat treated for 25 hours at

1300°C showed no trace of γ-alumina nor any amorphous silica phase, but instead showed a much higher content of α-alumina (Figure 2). The heat treatment at 1300°C was not performed for long enough to obtain the state of least energy, as can be seen by comparing the crystalline phase content of the HT 1300 and HT 1400 fibers (Figure 2). It is then expected that the mullite phase will dissociate until it achieves a state near the stoichiometric mullite structure: 72 wt% alumina and 28 wt% silica. This is the case for the HT 1400 fibers. The XRD measurements at elevated temperatures (shown in Figure 3B) showed that no transformation occurred during heating or after 8 hours at 1200°C, proving that the microstructure of the fibers is stable at those conditions. The alumina content of the mullite phase of the HT 1400 fibers at room temperature was determined to be 72.6 wt% based on the lattice parameters and the equation proposed by Fischer.[24] The microstructure of the HT 1400 fibers can be then considered to be the most stable.

Both aforementioned microstructural changes affected the creep behavior of the fibers, as shown in Figure 4. From the creep curves, it is possible to observe that the primary creep stage was shorter for the heat-treated fibers. During this stage, the initial strain rate is high and slowly decreases until reaching a constant value. Therefore, this stage is associated with the microstructural changes that occur under creep loading. The longer primary stage of the as-received fibers can then be related to their lower stability, i.e., more pronounced phase transformation at 1200°C, as shown in Figure 3A. Following this argument, the HT 1400 fibers showed only a very short primary stage since no phase transformation was detected, as shown in Figure 3B. In fact, the HT 1400 fibers were the only fibers to really achieve a steady-state creep stage. When a load is applied, the as-received fibers may show different phase transformation kinetics in comparison to the results of Figure 3. Still, it is expected that their microstructure will slowly change during the greater part of the creep tests. The same is valid for the HT 1200 fibers and possibly for the HT 1300 fibers. Given these continuous phase changes, the term minimum creep rate is then more accurate than steady-state creep rate for the two-phase oxide fibers.

During the creep tests, the creep rate was observed to decrease for the previously treated fibers. Although grain growth caused strength loss, it had a positive influence on the creep resistance. It is well known that bigger grains have a higher resistance against creep deformation.[25] Here, it should also be highlighted that the presence of the SiO_2 glass phase, even in small amounts, can also locally increase the creep deformation of the as-received fibers. This glassy phase is absent after thermal treatment.[18] As a consequence, the heat-treated fibers showed much smaller creep rates. For a better comparison, Figure 6 shows the minimum creep rates measured for the fibers under different applied stresses.

The values of the as-received Nextel 720 fibers[13] are also given, since this oxide fiber is credited to have the highest creep resistance. The low creep rates of Nextel 720 are a result of its microstructure of 0.5 μm mosaic mullite grains.[11] Nevertheless, the CeraFib 75 fibers heat treated at 1300°C and 1400°C showed even lower creep rates. However, it is expected that the Nextel 720 fibers would also show a decreased creep rate after similar thermal treatment. Moreover, the results could be fitted with the Arrhenius creep rate equation as in the following:

$$\dot{\varepsilon} = \frac{ADGb}{kT} \left(\frac{b}{d}\right)^p \left(\frac{\sigma}{G}\right)^n,$$

where $\dot{\varepsilon}$ is the creep rate, A is a dimensionless constant, D is the diffusion coefficient, G is the shear modulus, b is Burger's vector, k is Boltzmann's constant, T is the absolute temperature, d is the grain size, p is the inverse grain size exponent, σ is the applied stress and n is the stress exponent. At a constant temperature of 1200°C, the stress exponent n could be estimated for each fiber condition. The calculated n for the as-received CeraFib 75 was 2.9, and it changed to 3.2 for HT 1200 and 3.7 for HT 1300 and HT 1400. The inverse grain size exponent p was also estimated to be 3.0 by taking into account the grain size of the fibers before the creep tests (Figure 1) and the creep rates corrected for 150 MPa. Hence, the creep rate of the mullite fibers is rather dependent on the applied stress and grain size.

Considering the presence of free SiO_2,[18] the metastable structure (Figure 3A), and the absence of cavitations in the fracture surface (Figure 5A), it is here suggested that the main creep mechanism for the as-received fibers is related to grain-boundary sliding, assisted by the presence of the glassy phase. This conclusion agrees well with the observations of
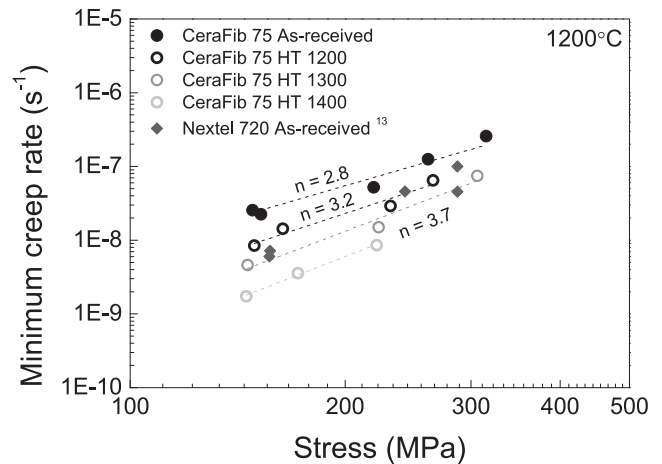

FIGURE 6 Minimum creep rate vs applied stress for the as-received CeraFib 75 fibers and the fibers after heat treatment for 25 hours at temperatures of 1200°C-1400°C. Data for the as-received Nextel 720[13] were included for comparison

Nextel 720, which presents *n*=3 at moderate stresses, and the creep mechanism is also related to grain-boundary diffusion, controlled by diffusion.[12] The shift in the stress exponent observed for the heat-treated fibers can be related to different creep deformation mechanisms occurring when the fibers are loaded. For mullite fibers, the relation between the creep mechanisms and the creep exponents can be problematic, given the complexity of the structure of the fiber, which are two-phase and fine-grained,[11,12] and they normally present stress exponents higher than bulky mullite materials. Furthermore, care should be taken when making direct comparisons of the measured exponents with creep mechanism and models proposed for other polycrystalline ceramics, as they are described for steady-state creep. As mentioned before, steady-state creep may not be achieved with two-phase fibers. Nonetheless, the evaluation of the creep exponents *n* and *p* can still be used to give a general idea of the possible creep mechanisms. For instance, $n \approx 4$ and $p \approx 3$ are normally related to grain-boundary sliding and cavity growth, according to the literature for polycrystalline ceramics.[26] From the observed microstructural changes and absence of the glassy phase, the grain mobility is found to be lower after thermal treatment. In this sense, the formation and growth of cavities, as shown in Figure 5C, begins to play a larger role in creep deformation. Therefore, the creep rate of the fibers is more sensitive to the applied stress, i.e., the increase in *n* observed for the HT 1300 and HT 1400 fibers.

In summary, the heat treatment of two-phase oxide fibers can be advantageous when a higher thermal stability is desired. In the literature, the effects of thermal exposure are normally only related to fiber degradation due to the strength decrease. However, heat treatments can be used to improve the fiber properties to a certain extent. Taking HT 1200 as an example, these fibers retained approximately 80% of the as-received strength but also showed a considerable improvement in creep resistance and creep lifetime, not to mention a more stable microstructure. It is important to highlight that the presented results can also be applied to other two-phase oxide fibers, such as Nextel 720, since it is expected that they will present similar microstructural changes after heat treatment due to their postprocessing metastable microstructure.[15,16,18,27,28] On the other hand, when the heat-treatment temperature is too high or the duration is too long, the achievement of higher thermal stability is not justified, as the strength decrease is too pronounced. For instance, HT 1400 did not show any further transformation at 1200°C, but the grain growth and fiber degradation was so high that the fiber could not be tested with the highest creep load. Still, this analysis shows that the mullite structure-containing 72.6 wt% alumina is stable at 1200°C. Hence, it is suggested that a pure mullite fiber with this composition would have a higher thermal stability than commercially available oxide fibers.

5 | CONCLUSIONS

In this study, the effect of different thermal exposures on the subsequent high-temperature behavior of mullite fibers was studied in detail. The studied material was CeraFib 75, a fiber that shows a metastable microstructure containing 175 µm mullite grains with traces of γ-alumina. Upon 25 hours of exposure to temperatures above 1200°C, grain growth and crystalline phase changes were detected. This led to a decrease in the room-temperature tensile strength but an increase in the thermal stability. The latter was analyzed by high-temperature XRD measurements and creep tests at 1200°C.

The kinetics of the phase transformations that occur in the fibers at 1200°C were quantified through XRD analysis. Changes in the phase content of the as-received fibers occurred during the first hours of exposure to 1200°C. First, the present γ-alumina phase combines with free silica to form mullite, and the overall content of the mullite phase in the fibers increases. Afterwards, the previously metastable mullite structure slowly dissociates into α-alumina grains and a mullite structure with lower Al content. After 25 hours of exposure to 1200°C, this reaction is not entirely complete, and therefore, the mullite phase content of the fiber further decreases when the fiber is heated again. These phase transformations occur at a faster pace at higher temperatures, e.g., 1300 and 1400°C. Particular attention was given to the fibers heat treated at 1400°C, since they did not present further transformation when exposed to 1200°C. These fibers showed a mullite structure containing 72.6 wt% alumina, which can then be considered stable at this temperature.

The effect of heat treatment on the creep behavior of the fibers was evident and could be related to the observed microstructural changes. In general, higher heat-treatment temperatures resulted in lower creep rates, a smaller primary creep stage, and an overall longer creep lifetime. This higher creep resistance of the fibers is due to the measured grain growth and higher thermal stability. In addition, since the fibers underwent phase transformation during the previous heat treatment, the overall creep deformation was considerably smaller. A possible change in the main creep mechanisms was also indicated in the fracture analysis. In this matter, it is suggested that the as-received fibers deformed mainly due to grain-boundary sliding, while cavity growth was more prominent in the heat-treated fibers. Nevertheless, the improvement in the thermal stability and creep properties came at the expense of the tensile strength. For the fibers heat treated at 1400°C, grain growth and degradation were so prevalent that the fibers could not be creep tested with loads higher than 220 MPa. It is then suggested that a pure mullite fiber containing 72.6 wt.% alumina would present better performance than the current oxide fibers. Attention should be given to grain growth when achieving this composition.

REFERENCES

1. Keller KA, Jefferson G, Kerans RJ. Oxide-Oxide Composites.in: Bansal NP, Lamon J, eds. *Ceramic Matrix Composites*. Hoboken, NJ: John Wiley & Sons, Inc., 2014, pp. 236-72

2. Noeth A, Rüdinger A, Pritzkow W. Oxide ceramic matrix composites – Manufacturing, machining, properties and industrial applications. *Ceram Appl*. 2015;3:48-54.

3. Zok FW. Developments in oxide fiber composites. *J Am Ceram Soc*. 2006;89:3309-3324.

4. Koch D, Tushtev K, Grathwohl G. Ceramic fiber composites: experimental analysis and modeling of mechanical properties. *Compos Sci Technol*. 2008;68:1165-1172.

5. Bunsell AR, Berger MH. Fine diameter ceramic fibres. *J Eur Ceram Soc*. 2000;20:2249-2260.

6. Deléglise F, Berger MH, Bunsell AR. Microstructural evolution under load and high temperature deformation mechanisms of a mullite/alumina fibre. *J Eur Ceram Soc*. 2002;22:1501-1512.

7. Volkmann E, Tushtev K, Koch D, Wilhelmi C, Göring J, Rezwan K. Assessment of three oxide/oxide ceramic matrix composites: mechanical performance and effects of heat treatments. *Compos Part A: Appl Sci Manufac*. 2015;68:19-28.

8. Antti ML, Lara-Curzio E, Warren R. Thermal degradation of an oxide fibre (Nextel 720)/aluminosilicate composite. *J Eur Ceram Soc*. 2004;24:565-578.

9. Ruggles-Wrenn MB, Musil SS, Mall S, Keller KA. Creep behavior of Nextel™610/Monazite/Alumina composite at elevated temperatures. *Compos Sci Technol*. 2006;66:2089-2099.

10. Ruggles-Wrenn M, Koutsoukos P, Baek S. Effects of environment on creep behavior of two oxide/oxide ceramic–matrix composites at 1200 C. *J Mater Sci*. 2008;43:6734-6746.

11. Wilson DM, Lieder SL, Lueneburg DC. Microstructure and high temperature properties of Nextel 720 fibers. pp. 1005-14. in Proceedings of 19th Annual Conference on Composites, Advanced Ceramics, Materials, and Structures. Edited by J. B. Wachtman Jr. John Wiley & Sons, Inc., 2008.

12. Armani CJ, Ruggles-Wrenn MB, Hay RS, Fair GE. Creep and microstructure of Nextel™ 720 fiber at elevated temperature in air and in steam. *Acta Mater*. 2013;61:6114-6124.

13. Almeida RSM, Tushtev K, Clauß B, Grathwohl G, Rezwan K. Tensile and creep performance of a novel mullite fiber at high temperatures. *Compos Part A: Appl Sci Manufac*. 2015;76:37-43.

14. Schmücker M, Flucht F, Mechnich P. Degradation of oxide fibers by thermal overload and environmental effects. *Mater Sci Eng: A*. 2012;557:10-16.

15. Petry MD, Mah T-I. Effect of thermal exposures on the strengths of Nextel™ 550 and 720 filaments. *J Am Ceram Soc*. 1999;82:2801-2807.

16. Deléglise F, Berger MH, Jeulin D, Bunsell AR. Microstructural stability and room temperature mechanical properties of the Nextel 720 fibre. *J Eur Ceram Soc*. 2001;21:569-580.

17. Hay RS, Boakye EE, Petry MD, Berta Y, Von Lehmden K, Welch J. Grain growth and tensile strength of 3M Nextel 720™ after thermal exposure. pp. 153-63. in Proceedings of 23rd Annual Conference on Composites, Advanced Ceramics, Materials, and Structures. Edited by E. Ustundag and G. Fischman. John Wiley & Sons, Inc., 2008.

18. Almeida RSM, Bergmüller EL, Eggert BGF, et al. Thermal exposure effects on the strength and microstructure of a novel mullite fiber. *J Am Ceram Soc*. 2016;99:1709-1716.

19. Goldsby JC, Yun HM, Morscher GN, DiCarlo JA. Annealing effects on creep of polycrystalline alumina-based fibers. *Mater Sci Eng: A*. 1998;242:278-283.

20. Hammond VH, Elzey DM. Comparing the creep response of alumina tows and single filaments. *Scripta Mater*. 2002;46:287-291.

21. Morrell R. A tensile creep-testing apparatus for ceramic materials using simple knife-edge universal joints. *J Phys E: Sci Instrum*. 1972;5:465.

22. Schmücker M, Schneider H, Mauer T, Clauβ B. Temperature-dependent evolution of grain growth in mullite fibres. *J Eur Ceram Soc*. 2005;25:3249-3256.

23. Schaper H, Van Reijen L. A quantitative investigation of the phase transformation of gamma to alpha alumina with high temperature DTA. *Thermochim Acta*. 1984;77:383-393.

24. Fischer RX, Schneider H, Voll D. Formation of aluminum rich 9:1 mullite and its transformation to low alumina mullite upon heating. *J Eur Ceram Soc*. 1996;16:109-113.

25. Cannon WR, Langdon TG. Creep of ceramics – Part 1. Mechanical characteristics. *J Mater Sci*. 1983;18:1-50.

26. Bernard-Granger G, Guizard C, Duclos R. Compressive creep behavior in air of a slightly porous as-sintered polycrystalline α-alumina material. *J Mater Sci*. 2007;42:2807-2819.

27. Schmücker M, Flucht F, Schneider H. High temperature behaviour of polycrystalline aluminosilicate fibres with mullite bulk composition. I. Microstructure and strength properties. *J Eur Ceram Soc*. 1996;16:281-285.

28. Wang Y, Cheng H, Liu H, Wang J. Microstructure and room temperature mechanical properties of mullite fibers after heat-treatment at elevated temperatures. *Mater Sci Eng: A*. 2013;578:287-293.

SUPPORTING INFORMATION

Additional Supporting Information may be found online in the supporting information tab for this article.